Results in Physics 17 (2020) 103044

Contents lists available at ScienceDirect

Results in Physics

journal homepage: www.elsevier.com/locate/rinp

Microarticle

Non-adiabatic reflection of particles in a multipole plasma trap configuration

N.K. Hicks[a,*], D.C. Massin[b]

[a] University of Alaska Anchorage Dept. of Physics & Astronomy, United States
[b] University of Alaska Anchorage College of Engineering, United States

ARTICLE INFO

Keywords:
Multipole plasma trap
Charged particle trap
Fermi acceleration
Anomalous heating
Collisionless heating

ABSTRACT

Charged particles incident on a region of time-varying, spatially inhomogeneous electric field may be reflected back toward the region of weaker field. This effect is used for adiabatic particle confinement in charged particle traps, but it may also be subject to non-adiabatic reflection that increases the particle energy. The electrons of a plasma in a multipole plasma trap may be heated by this effect. This work explores the energy gain of electrons in such a device with parameters relevant to laboratory experimentation, and it presents in one representative case an average 10% energy gain after a single reflection.

Introduction

An electric field of the form $\mathbf{E}_0(\mathbf{r})\cos(\Omega t)$exerts a time-averaged force on charged particles toward regions of weaker field. This is expressed as the ponderomotive force [1,2] on a particle of charge q and mass m:

$$\mathbf{F}_p = -\frac{q^2}{4m\Omega^2}\nabla\mathbf{E}_0^2$$

In particular, with the proper choice of field parameters, a multipole electric field can trap charged particles in 2D or 3D [3–5]. A 2D multipole trap, or radio frequency (RF) linear trap, of order N has 2 N electrodes with voltage $V(t) = \pm V_{rf}\cos(\Omega t)$ applied to them (with adjacent electrodes having opposite polarity), and radial distance r_0 from trap center to electrode surface (an example is shown in Fig. 1). The 2D multipole field magnitude is

$$|E_0| = \frac{V_{rf}}{r_0}N\left(\frac{r}{r_0}\right)^{N-1}$$

and particle trajectories generally remain stable as long as the particle interaction with the electric field is adiabatic: $|2(\mathbf{a}\nabla)\mathbf{E}_0| < |\mathbf{E}_0|$, where $\mathbf{a}$ is the amplitude of the particle oscillation at Ω, such that they do not gain significant kinetic energy from the trapping field over the period of field oscillation. An adiabaticity parameter η has been defined and found empirically [6] to satisfy the adiabaticity requirement when

$$\eta = \frac{|2(\mathbf{a}\nabla)\mathbf{E}_0|}{|\mathbf{E}_0|} = \frac{2q\ |\nabla\mathbf{E}_0|}{m\Omega^2} < 0.3$$

and, for the multipole field, this becomes

$$\eta(r) = \frac{2N(N-1)qV_{rf}}{m\Omega^2 r_0^2}\left(\frac{r}{r_0}\right)^{N-2} < 0.3$$

If a particle traverses a region of the trap where $\eta > 0.3$, it may gain kinetic energy; if it gains sufficient kinetic energy, it will ultimately exit the trap or collide with its electrodes. However, having $\eta > 0.3$ near the trap boundary does not mean that the particle will absolutely be lost on its first encounter with the boundary. It may instead be reflected by the ponderomotive barrier (in the adiabatic approximation this is represented by an effective potential well [7]). The *non*-adiabatic process [8] is related to that of Fermi acceleration [9–11], which has the mechanical analogy of a billiard ball encountering a vibrating wall (the ball may rebound from the wall with increased energy). If this process occurs, for example, in a multipole plasma trap device [12,13], and if the plasma conditions are such that the reflected, accelerated particle experiences a mean free path for collisions small compared to the device size, then the fast particle may thermalize. The particle transfers energy to the bulk plasma, and itself returns to an energy at which it is unlikely to be lost at its next encounter with the trap boundary. In this way, the plasma temperature will gradually increase, and the non-adiabatic acceleration of particles at the boundary does not lead to prompt particle loss. The purpose of this article is to present this concept as an extension of standard adiabatic multipole plasma trap research and to make an initial exploration of the concept with trap

* Corresponding author at: University of Alaska Anchorage Dept. of Physics & Astronomy, 3101 Science Circle, Anchorage, AK 99508, United States.
E-mail address: nkhicks@alaska.edu (N.K. Hicks).

https://doi.org/10.1016/j.rinp.2020.103044
Received 22 June 2019; Received in revised form 27 January 2020; Accepted 2 March 2020
Available online 04 March 2020

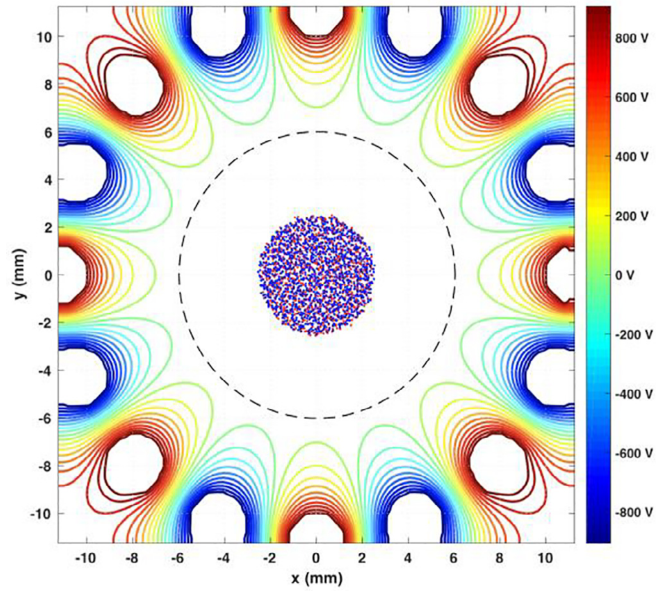

Fig. 1. Electric potential contours of an $N = 8$ linear multipole plasma trap of radius $r_0 = 10$ mmand RF voltage $V_{rf} = 1000$ V. The 16-pole trap has a "field-free" region of $E(r)/E(r_0) < 3\%$denoted by the dashed circle. When positive and/or negative particles are loaded into the trap center as shown, their subsequent transverse motion is constrained and bounded in the region of strong trapping field.

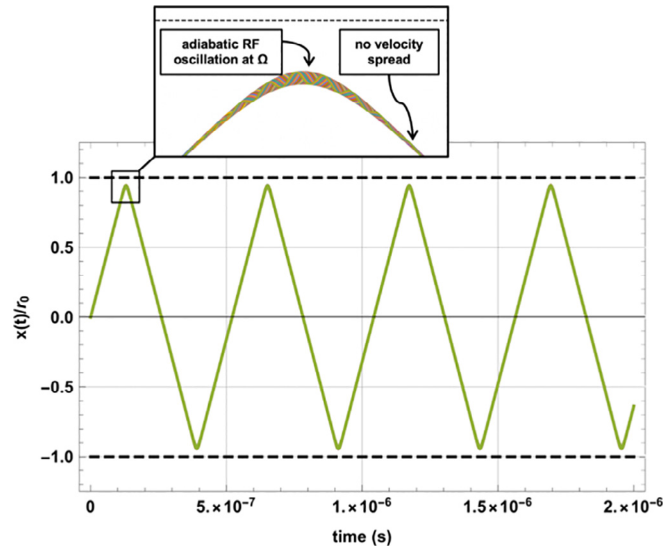

Fig. 2. Trajectories (position normalized to trap radius) of 18 electrons released from the origin with initial energy 10 eV in the 32-pole trap with adiabatic trap parameters (500 RF periods elapse). Particle trajectories depend negligibly on the electric field phase ϕ; therefore, trajectories overlap, and particle energies after reflection have not changed. The inset shows the envelope and individual trajectories during reflection, illustrating the high-frequency oscillation at the trap frequency Ω. The trap boundary (position of electrode tips) is denoted by black dashed lines.

conditions relevant to a laboratory experiment. This first step is to investigate the spectrum of energies at which an incoming particle will be reflected from a multipole plasma trap boundary, as a precursor to possible future in-depth computational or experimental study of the concept.

Methods and results

Particle trajectories are calculated numerically using Mathematica NDSolve to solve the 2D multipole equation of motion:

$$\ddot{x}(t) = -N\frac{q}{m}\frac{V_{rf}}{r_0}\sin(\Omega t + \phi)\left(\frac{x}{r_0}\right)^{N-1}$$

for motion that occurs along the x-axis only (with zero initial y-position and y-velocity, the particle ideally remains on the x-axis). Field parameters appropriate for an envisioned experimental multipole plasma trap apparatus are used as a starting point. The device is a 32-pole trap with $r_0 = 25.0$ cm, $f_{rf} = \Omega/2\pi = 250$ MHz, and $V_{rf} = 1000$ V. Only electron motion is considered, since ions are too massive to respond strongly given these field parameters. As a test of the method, electrons with kinetic energy 10 eV are launched from the origin. With these trap parameters, for electrons the trap has $\eta \leqslant 0.3$for $r \leqslant 24.0$ cm, and an effective potential well depth of 20 eV, so it is expected that the 10 eV electrons will be repeatedly, adiabatically reflected. This is confirmed as shown in Fig. 2, which also shows the detailed high frequency oscillation during reflection for 18 trajectories experiencing different phases ϕ of the electric field.

To investigate non-adiabatic reflection, energy gain, and acceleration dependence on ϕ, the trap parameters are adjusted such that, at the location in the trap where $\eta \leqslant 0.3$, the effective potential well depth is lower than the incident electron energy. With a deliberate choice of parameters, electrons access a strong enough field gradient to be accelerated upon reflection, and yet cannot reach the trap boundary. In particular, we reduce the driving frequency to $f_{rf} = 100$ MHz, and raise the RF voltage to $V_{rf} = 1250$ V. The resulting electron trajectories are shown in Fig. 3.

The variation in ϕ for the electrons results in differing acceleration

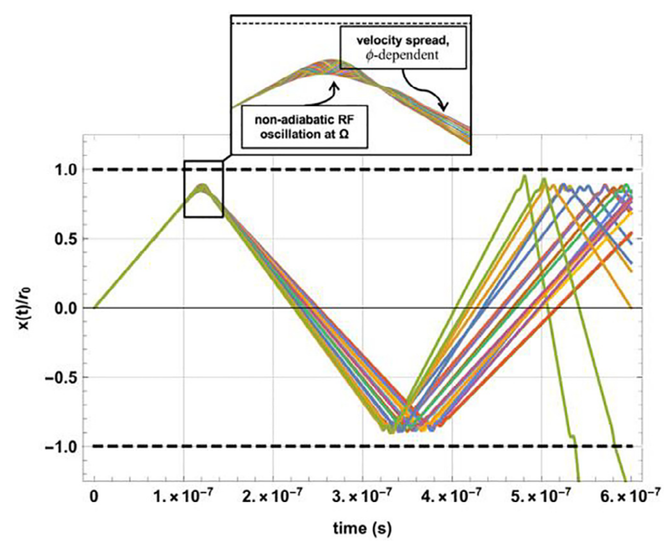

Fig. 3. 10 eV electron trajectories in the non-adiabatic multipole field (60 RF periods elapse). The variation in ϕ leads to a range of acceleration experienced by the particles during reflection. All particles remain in the trap for the first three reflections regardless of phase; the fastest particles are lost after the third reflection.

upon reflection, as can be interpreted from the outgoing slopes of the trajectories after reflection. This is further illustrated in Fig. 4, which shows the kinetic energy of each electron. After the first reflection, there is some increase and some decrease in individual particle energies; however, the average energy has increased significantly, as is consistent with a Fermi acceleration process. In this case, the average energy gain is 10%. In the second reflection, the fastest particles penetrate more deeply into the strong field region, leading to a further spread in outgoing velocities. The resulting average energy gain is 13%. Fig. 4 also shows the average energy gain of electrons of varying incident energy, with the maximum energy chosen to be the highest

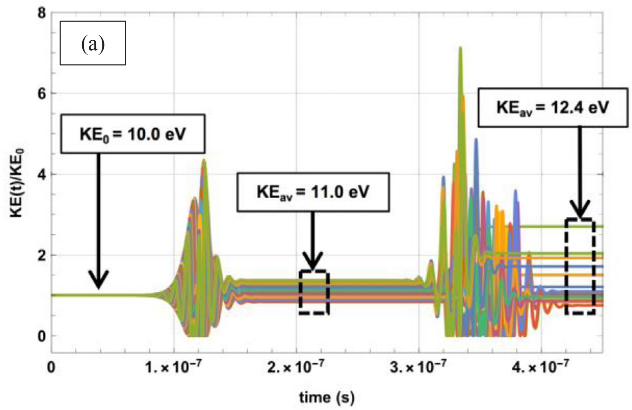

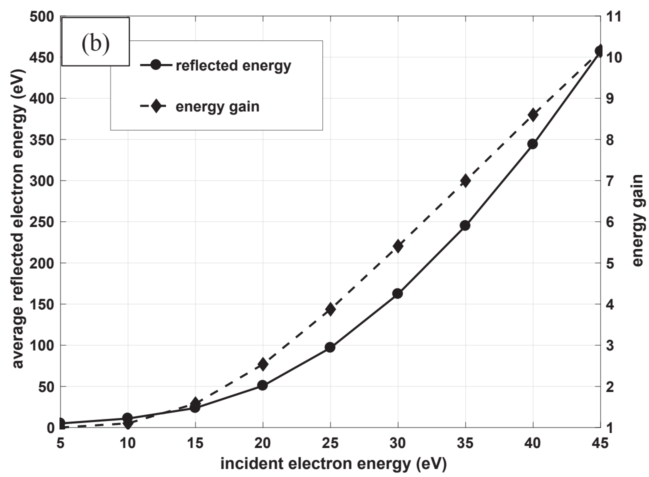

Fig. 4. (a) Electron kinetic energies (normalized to initial energy) for the trajectories in Fig. 3 (the first 45 RF periods are shown). The average kinetic energy of the 18 trajectories is shown for three times: before reflection; after first reflection; after second reflection. Individual kinetic energies fluctuate strongly during each reflection but remain constant while particles traverse the field-free region. (b) Average energy and energy gain after a single reflection of electrons with incident energies ranging from 5 to 45 eV are shown. 45 eV is the highest incident energy for which no electrons are lost during the reflection.

energy at which no particles are lost during the reflection.

Conclusions and discussion

The possibility of accelerating charged particles that approach the boundary of a multipole plasma trap configuration has been presented. The trap parameters are adjusted to make the particle interaction with the electric field non-adiabatic, yet particles are reflected back into the trap before encountering the trap boundary. For brevity, a single representative example of a multipole plasma trap tuned for non-adiabatic reflection of 10 eV electrons at all incoming phases with respect to the electric field has been illustrated: the electrons experience a 10% average energy gain after one reflection. The example given also indicates that more energetic particles can still be reflected, with correspondingly higher energy gain due to deeper penetration into the non-adiabatic field region. In this example, 45 eV electrons experience an energy gain 100 times larger than the 10 eV electrons. It is expected that the 1D case presented illustrates a "worst case" for potential particle loss, since particles traveling directly toward a multipole electrode tip have the greatest possible spread in reflected energy as a function of RF phase. To confirm this, the same multipole plasma trap configuration was also analyzed in 2D (again using Mathematica NDSolve), this time employing the order-16 Cartesian multipole potential [14]:

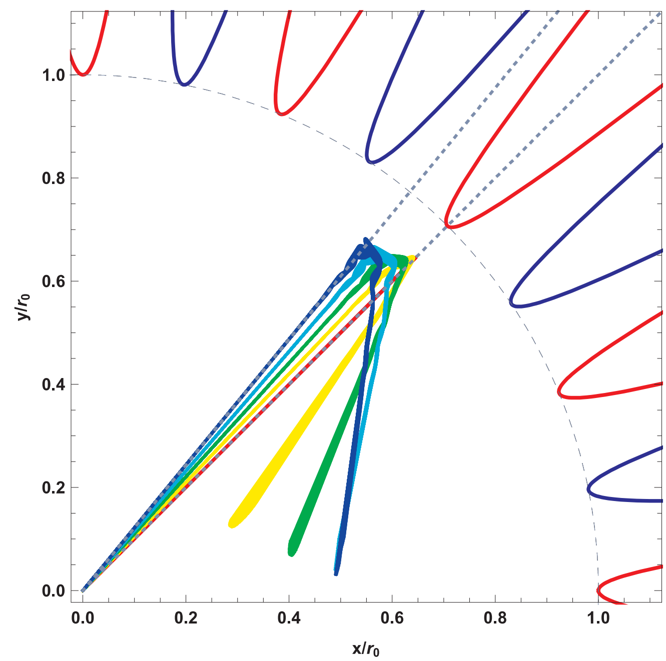

Fig. 5. 2D electron trajectories (20 RF periods elapse) at various launch angles for the non-adiabatic multipole field (same multipole parameters as the case in Fig. 3). The ideal hyperbolic electrode shapes of alternating polarity are shown in red and blue. The dashed line shows the trap aperture r_0. 90 electrons (uniformly sampling initial RF phase ϕ between π/2 and 3π/2) at each of 5 launch angles are tracked, with initial energy 10 eV, and with the trajectories showing that all 450 particles are reflected and none are lost. The range of launch angles is bounded by the dotted lines.

$$V(x, y, t) = \frac{V_{rf}\sin(\Omega t + \phi)}{r_0^{16}}[x^{16} + y^{16} - 120(x^{14}y^2 + x^2y^{14}) + 1820(x^{12}y^4 + x^4y^{12}) - 8008(x^{10}y^6 + x^6y^{10}) + 12,870x^8y^8]$$

The results are shown in Fig. 5, which demonstrates the reflection of 450 electrons at 10 eV (at a range of launch angles spanning 1/2 the angular separation between poles, and with a range of initial RF phase ϕ from π/2 to 3π/2). This distribution of launch angles and phases covers the range of RF multipole field conditions that particles originating at the trap center can encounter when approaching the 2D trap boundary (adding trajectories for more launch angles or initial RF phases does not show results that deviate from these). Further work can involve investigation of tuning field parameters to adjust the energy gain, and particle-in-cell plasma simulation can explore the heating effect over a broad trap parameter space, and also with variation of the incident particle distribution. The results presented here and to be determined in follow-on work will inform the experimental investigation of this heating effect in the multipole plasma trap. The scaling of trap and plasma parameters to account for the possible collisionless heating of edge particles and subsequent collisional heating of the bulk plasma by these particles will be investigated.

Declaration of Competing Interest

The authors declare that they have no known competing financial interests or personal relationships that could have appeared to influence the work reported in this paper.

Acknowledgments

This work is supported by U.S. National Science Foundation grants PHY-1619615 and PHY-1806113. D. Massin is supported by an Alaska

Space Grant Undergraduate Research Fellowship.

Appendix A. Supplementary data

Supplementary data to this article can be found online at https://doi.org/10.1016/j.rinp.2020.103044.

References

[1] Kapitza PL. Sov. Phys. JETP 1951;21:588.
[2] Lichtenberg AJ, Lieberman MA. Regular and Chaotic Dynamics. second ed. New York, New York, NY: Springer; 1992.
[3] Gerlich D. Phys. Scr. 1995;T59:256.
[4] Walz J, Siemers I, Schubert M, Neuhauser W, Blatt R, Teloy E. Phys. Rev. A 1994;50:4122.
[5] Niculae CM. Europhys. Lett. 1998;43:398.
[6] D. Gerlich, in Adv. Chem. Phys. State-Selected State-To-State Ion-Molecule React. Dyn. Part 1. Exp. Vol. 82, C.-Y. Ng, M. Baer (Eds.) (John Wiley & Sons, Inc, 1992), pp. 1–176.
[7] Landau LD, Lifshitz EM. Theoretical Physics Vol. 1. Oxford: Pergamon; 1960.
[8] Dodin IY, Fisch NJ. Phys. Plasmas 2007;14:055901.
[9] Fermi E. Phys. Rev. 1949;75:1169.
[10] Lieberman MA, Godyak VA. IEEE Trans. Plasma Sci. 1998;26:955.
[11] Shah K, Ramachandran H. Phys. Plasmas 2008;15:062303.
[12] Hicks NK, Zaki M, Mojica M, Hamlin I, Renner P, Stassel B. Results Phys. 2019;15:102568.
[13] Hicks NK, Bowman A, Godden K. Physics 2019;1:392.
[14] Szilagyi M. Electron and Ion Optics. US, Boston, MA: Springer; 1988.